

Hardness of Nanostructured Al–Zn, Al–Mg and Al–Zn–Mg Alloys Obtained by High-Pressure Torsion

A.A. Mazilkin^{1,a}, B. Baretzky^{2,b}, S. Enders^{2,c}, O.A. Kogtenkova^{1,d},
B.B. Straumal^{1,2,e}, E. Rabkin^{3,f} and R.Z. Valiev^{4,g}

¹Institute of Solid State Physics, RAS, Chernogolovka, Moscow district, 142432 Russia

²Max-Planck-Institut für Metallforschung, Heisenbergstrasse 3, 70569 Stuttgart, Germany

³TECHNION-Israel Institute of Technology, 32000 Haifa, Israel

⁴Ufa State Aviation Technical University, 450000 Ufa, Russia

^amazilkin@issp.ac.ru, ^bbaretzky@mf.mpg.de, ^cenders@mf.mpg.de, ^ekoololga@issp.ac.ru,
^estraumal@issp.ac.ru, ^ferabkin@technion.ac.il, ^grzvaliev@mail.rb.ru,

Keywords: high pressure torsion; nanocrystalline materials; enhanced diffusion; nanohardness

Abstract. Microstructure and hardness of ternary Al–Zn–Mg alloys were studied both in as cast state and after high pressure torsion (HPT) with 5 torsions (shear strain about 6). The size of (Al) grains and of reinforcing second phase precipitates decreases drastically after HPT reaching nanometer range. During HPT, the Zn- and Mg-rich supersaturated (Al) solid solution decomposes and reaches the equilibrium state corresponding to the room temperature. In the as cast state the hardness of the supersaturated solid solutions increases with increasing Zn and Mg content due to the solid-solution hardening. However, after HPT the work hardening and Hall-Petch hardening due to the decreasing grain size competes with softening due to the decomposition of a supersaturated solid solution. In the net effect, the severe plastic deformation results in softening of ternary Al–Zn–Mg alloys.

Introduction

The manufacturing of materials with a very small grain size in nanometer range is an important way for improving the mechanical properties of metallic materials [1]. Very promising from this point of view are the techniques of severe plastic deformation (SPD). The SPD techniques, namely equal channel angular pressing (ECAP) and high pressure torsion (HPT) do not involve changes in the material geometry, in contrast to the conventional processes of high deformation like rolling or wire drawing. However, the processes of structural changes during SPD are very complicated and have not been yet fully understood.

In our previous works the severe plastic deformation of binary Al–Zn, Al–Mg and ternary Al–Zn–Mg alloys have been studied [2, 3]. It has been demonstrated that as a result of HPT, the Zn-rich (Al) supersaturated solid solution decomposes completely and reaches the equilibrium state corresponding to the room temperature. The decomposition is less pronounced for Al–Mg and Al–Mg–Zn alloys. We concluded that the severe plastic deformation of supersaturated solid solutions could be considered as a balance between deformation-induced disordering and deformation-accelerated diffusion bringing the alloys closer to the equilibrium. It is the well-known fact that the increase of the concentration of solute component leads to the solid solution hardening of a material. On the other hand, the decrease of grain size leads to the Hall-Petch hardening. Based on our previous results [2, 3] it can be expected that both processes compete during HPT. It has been shown recently that SPD may lead to materials softening since the needles of hardening phase break during ECAP [4]. The study of the effect of HPT on the hardness of ternary Al–Zn–Mg alloys is the main goal of the present work.

Experimental

Aluminium based alloys of the following compositions were investigated (the alloys content is indicated in weight percents): Al with 5%Zn–2%Mg and 10%Zn–4%Mg. The alloys were prepared of high purity components (5N5 Al, 5N Zn and 4N5 Mg) by vacuum induction melting. As-cast disks of these alloys obtained after grinding, sawing and chemical etching were subjected to HPT at room temperature under the pressure of 5 GPa in a Bridgman anvil type unit (5 torsions, duration of process about 300 s) [5]. All samples for the investigations were cut from the deformed disks at a distance of 5 mm from the sample centre. For this distance the shear strain is ~ 6 . Transmission electron microscopy (TEM) investigations have been carried out in a JEM–4000FX microscope at an accelerating voltage of 400 kV. X-ray diffraction (XRD) data were obtained on a SIEMENS–500 diffractometer ($\text{CuK}\alpha_1$ radiation) with a graphite monochromator and line position sensitive gas flow detector. The hardness measurements were performed using a Nanoindenter by the Nano Instruments, Inc., Knoxville, TN. The system has load and displacement resolution of 0.3 μN and 0.16 nm respectively. A Berkovich indenter, a three-sided pyramid with an area-to-depth function which is the same as that of a Vickers indenter, was used. The system was thermally buffered and the temperature of surrounding was controlled within $\pm 1^\circ\text{C}$. Six indentations were made for each specimens and results presented here are averages for the group. Specimens were loaded up to 60–70 mN. The dimension of the indentation imprints was about 10–12 μm .

Results and Discussion

Al–Zn–Mg coarse-grained alloys (as cast state prior to HPT deformation) contain grains of two phases (Fig. 1). These are (Al) solid solutions with a mean size of 500 μm and colonies of interme-

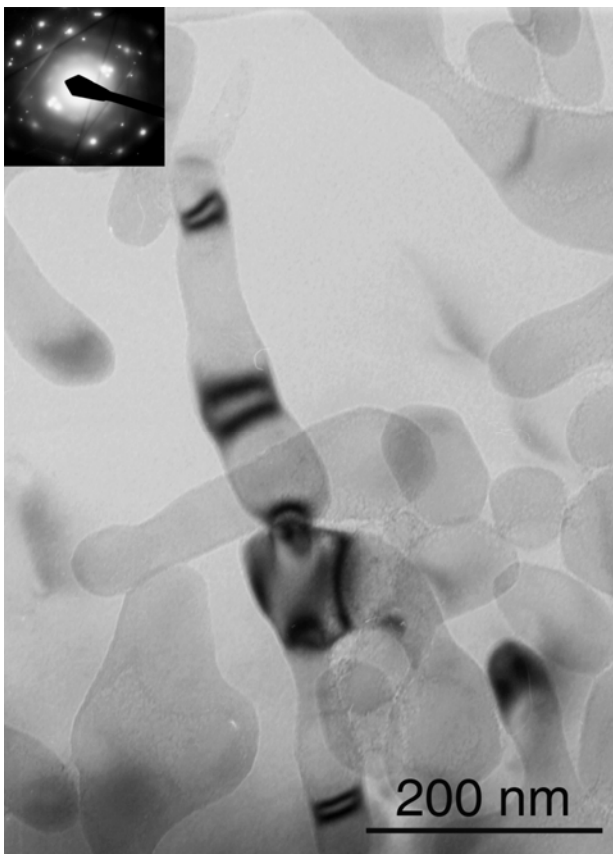


Fig. 1a Microstructure of coarse grained Al–5%Zn–2%Mg alloys (as cast state)



Fig. 1b Microstructure of coarse grained Al–10%Zn–4%Mg alloys (as cast state)

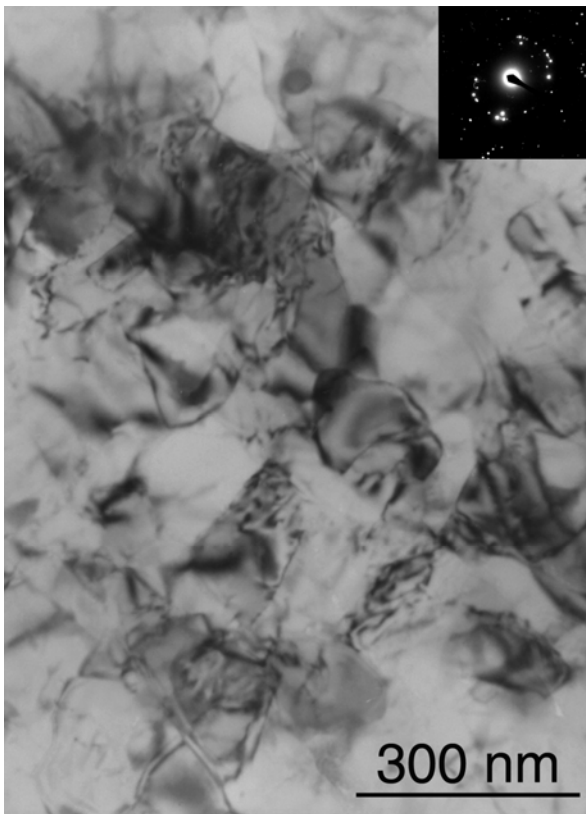


Fig. 2a Microstructure of fine grained Al-5%Zn-2%Mg alloys (after HPT)

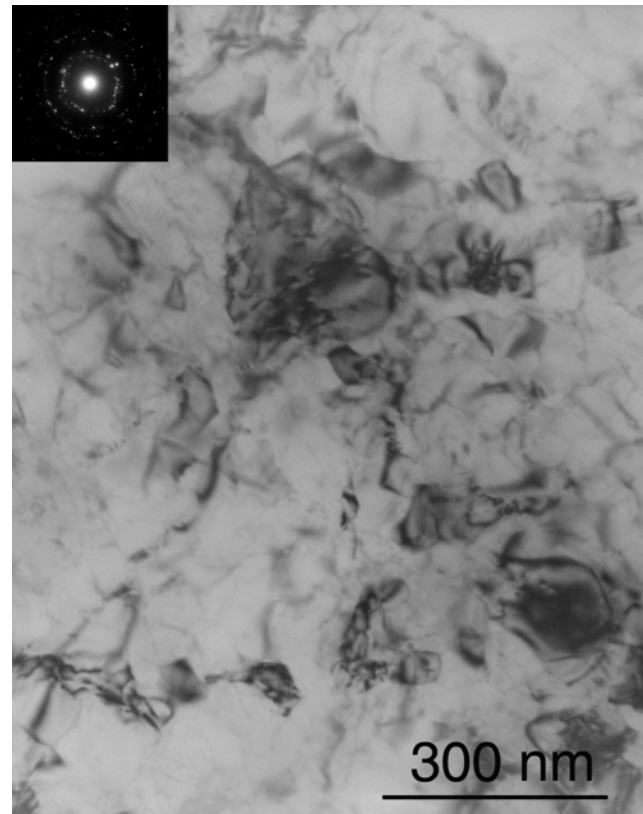


Fig. 2b Microstructure of fine grained Al-10%Zn-4%Mg alloys (after HPT)

tallic $\text{Mg}_{32}(\text{ZnAl})_{39}$ τ -phase. Colony size was about 500 nm. The dislocation density in (Al) is $\sim 10^{12} \text{ m}^{-2}$. XRD data do not reveal the presence of τ phase in the alloys, which means that its volume fraction is less than 1%.

The microstructures of Al-Zn-Mg alloys after HPT deformation (Fig. 2) exhibit (Al) grains with the mean size of 150 nm (Al-5%Zn-2%Mg) and 120 nm (Al-10%Zn-4%Mg). Dislocations are observed to be mainly arranged in subgrain boundaries. Selected area diffraction (SAED) patterns revealed the presence of the τ -phase particles. They are uniformly distributed in the material. The particles of the τ -phase are extremely dispersed. They are not distinguished in the conventional TEM micrographs and they were detected only by the additional spots in the electron diffraction patterns. The grain sizes of the τ phase can be estimated to be ~ 10 nm. X-ray analysis did not detect the secondary phases.

It is known that both small grain size (less than 500 nm) and internal stress contribute to X-ray line broadening. The method to separate these contributions is known as Williamson-Hall procedure [5]. The procedure was modified by T. Ungar et al. [6, 7]. This procedure was applied in [2] in order to measure the dislocation density after HPT. In Mg-containing alloys it increases during HPT up to $10^{15} - 10^{16} \text{ m}^{-2}$.

In Fig. 3 the microhardness of Al-Zn-Mg alloys in the as cast state and after HPT is shown. In the coarse-grained as cast alloys the dimension of the indentation imprints was lower than grain size. The hardness grows with increasing content of Mg (and Zn) both in as cast state and after HPT. In as cast state both Al-5%Zn-2%Mg and Al-10%Zn-4%Mg alloys contain almost exclusively supersaturated solid solution with very small ($< 1\%$) amount of τ -phase $\text{Mg}_{32}(\text{ZnAl})_{39}$. Supersaturation of solid solution in Al-5%Zn-2%Mg and Al-10%Zn-4%Mg alloys in as cast state is rather high, since equilibrium solubility of Zn and Mg in Al at room temperature is below 1 wt. % [8]. Therefore, the increase of hardness of Al-Zn-Mg alloys with increasing amount of alloying elements Zn and Mg may be attributed mainly to the solid-solution hardening. The increase of shear

stress with increasing content of alloying element in a solid-solution is well-known known for the metals with face-centred cubic (fcc) lattice since pioneering works [9, 10].

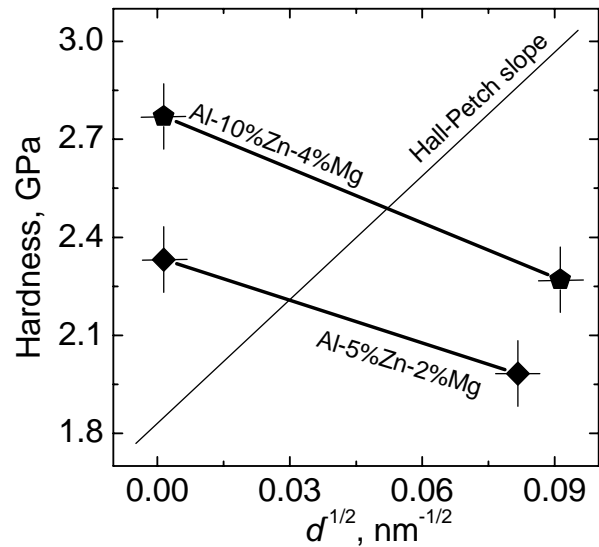
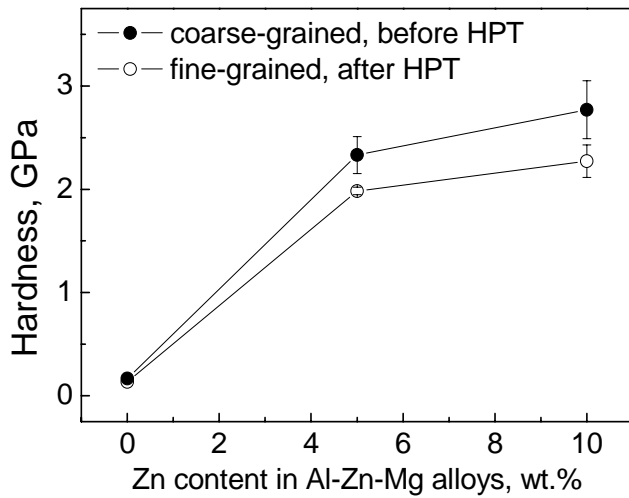


Fig. 3 Microhardness of Al-Zn-Mg alloys before and after high pressure torsion

Fig. 4 Dependence of microhardness on grain size d in Hall-Petch coordinates

In sharp contrast with the expectations based on Hall-Petch model the hardness of Al-Zn-Mg alloys decreases substantially after HPT. It happens in spite of the definite work hardening during the HPT: the dislocation density increased in Al-based solid solution from 10^{12} m^{-2} to $10^{15} - 10^{16} \text{ m}^{-2}$. Also, in the fine-grained alloys after HPT the dimensions of the indentation imprints are much higher than the grain size, since the grain size decreased drastically after HPT (Fig. 4). It means that the measured microhardness value includes the grain boundary Hall-Petch input. However, the microhardness dependence on the grain size does not follow the expected Hall-Petch behaviour [11, 12] (see Fig. 4). In other words, the softening input during HPT prevails over the work hardening (due to the increase of dislocation density) and Hall-Petch hardening (due to the decrease of grain size). What is the possible reason of the observed softening during HPT?

In previous works we observed that in Al-Zn, Al-Mg and Al-Zn-Mg alloys the supersaturated solid solution (Al) decomposes into equilibrium phases [2, 3]. The Zn-rich supersaturated solid solution (Al) decomposes completely and reaches the equilibrium corresponding to the room temperature. This process is less pronounced for the Mg-rich (Al) solid solution. It has been observed that the lattice parameter a both in Al-Zn and Al-Mg alloys increases after HPT deformation, therefore, recovering to a value close to that of pure Al. However, in Al-Mg alloys such recovery is much less pronounced. Therefore, HPT results in the formation of a phase structure which is closer to the equilibrium state than that of the initial coarse grained material. In terms of decomposition of the supersaturated solid solution the ternary Al-Zn-Mg alloys occupy an intermediate position between Al-Zn and Al-Mg alloys [3]. The supersaturated solid solution (Al) containing both (Zn) and (Mg) decomposes substantially, though to a lesser extent than in case of Al-Zn alloys without Mg.

One can estimate the input of various diffusion mechanisms into decomposition of supersaturated (Al) solid solutions in Al-Zn-Mg alloys. The supersaturation is the driving force for the bulk diffusion of Zn and Mg from the solid solution to the sinks (GBs or particles of β and τ phases). The diffusion paths for individual Zn and Mg atoms would be about 500 nm in this case. It corresponds to the bulk diffusion coefficients of $10^{-17} \text{ m}^2 \text{ s}^{-1}$. The available data for bulk diffusion of Zn in Al give the values of D (300 K) $\approx 1.0 \cdot 10^{-22} \text{ m}^2 \text{ s}^{-1}$ [13, 14]. Extrapolation of the data for Mg bulk diffusion in Al single crystals gives D (300 K) $\approx 1.7 \cdot 10^{-24} \text{ m}^2 \text{ s}^{-1}$ [15]. Both values are about 8

orders of magnitude lower than those estimated from the diffusion path of the actual solid-solution decomposition during HPT. Therefore, the bulk diffusion can be considered as frozen and cannot ensure the decomposition of solid solution during HPT.

The transport of Zn and Mg from the (Al) matrix can be controlled by grain boundary diffusion of Zn atoms along (Al) GBs. Indeed, the solute solution hardening of (Al) matrix by Zn and Mg implies that there is a strong attractive interaction between these impurity atoms and the dislocation cores in the matrix. Since the re-arrangement and self-organisation of dislocation substructure is a probable formation mechanism of the new GBs during HPT, these newly formed GBs will be heavily enriched by Zn and Mg. The diffusion of Zn and Mg toward growing precipitates will occur then in the GBs rather than in the bulk. Taking into account the possible diffusion path (~500 nm) and time of the process (300 s) the estimation yields a $D\delta$ value of $10^{-24} \text{ m}^3\text{s}^{-1}$ for a GB thickness of $\delta = 0.5 \text{ nm}$. Extrapolation of data [16] ^{65}Zn tracer GB diffusion to 300 K yields the value of $sD\delta = 3 \cdot 10^{-24} \text{ m}^3\text{s}^{-1}$ that is close to our estimation. A similar value of $sD\delta = 10^{-23} \text{ m}^3\text{s}^{-1}$ is obtained also from [17–19]. Therefore, the GBs in Al provide the diffusion paths for Zn which can be responsible for the decomposition of supersaturated solid solution during HPT. The extrapolation of the data for Mg GB diffusion in Al obtained in [20, 21] to 300 K yields $sD\delta$ value of $5 \cdot 10^{-28} \text{ m}^3\text{s}^{-1}$. These data demonstrate undoubtedly a lower GB diffusivity of Mg in comparison with Zn. This fact explained the slower decomposition of supersaturated solid solutions in Al–Mg and Al–Zn–Mg alloys in comparison with Al–Zn alloys deformed in the same HPT conditions [2, 3]. Nevertheless, both Zn and Mg GB diffusivities extrapolated towards 300 K are much higher than the $sD\delta$ value for the Al GB self-diffusion ($10^{-31} \text{ m}^3\text{s}^{-1}$ [18]).

Therefore, the GB diffusion can explain the partial decomposition of supersaturated (Al) solid solutions in Al–Zn–Mg alloys. As a result of HPT, the partial decomposition of supersaturated (Al) solid solution decreases the solid solution hardening in (Al) matrix. This decrease is stronger than the work hardening (due to the increase of dislocation density), the Hall-Petch hardening (due to the decrease of grain size) and the precipitation hardening (due to the increase in dispersion of the second phase precipitates). Therefore, in this work the another softening mechanism during SPD (in addition to the break of hardening needle-like particles observed in [4]) has been observed. It means that the severe plastic deformation does not automatically lead to the hardening of a treated material.

Conclusions

1. Severe plastic deformation by HPT of ternary Al–Zn–Mg alloys leads to a strong decrease of the size of (Al) and (Zn) grains (below 100 nm) and of particles of reinforcing phases (below 10 nm). Therefore, HPT produces the nanostructures which are further away from the equilibrium state than the initial coarse grained material. At the same time, during HPT the Zn- and Mg-rich supersaturated solid solution (Al) decomposes and approaches the phase equilibrium state corresponding to the room temperature. Therefore, HPT results in the formation of a phase structure which is closer to the equilibrium state than that of the initial coarse grained material. The most probable mechanism of the equilibration of the (Al) supersaturated solid solution is grain boundary diffusion accelerated by fluxes of vacancies produced due to the SPD.
2. In the as cast state the hardness of the supersaturated solid solutions increases with increasing Zn and Mg content due to the solid-solution hardening. However, after HPT the work hardening and Hall-Petch hardening due to the decreasing grain size competes with softening due to the decomposition of a supersaturated solid solution. In the net effect, the severe plastic deformation results in a softening of ternary Al–Zn–Mg alloys.

Acknowledgements

The investigations were partly supported by the German Federal Ministry for Education and Research (contract RUS 04/014), INTAS (contract 03-51-3779), Russian Foundation for Basic Research (contracts 03-02-16947 and 04-03-34982) and Israeli Center for Academic Relations with the CIS and Baltic States (Hebrew University, Jerusalem).

References

- [1] R. Valiev: *Nature Mater.* Vol. 3 (2004), p. 511; *Nature* Vol. 419 (2002), p. 887
- [2] B.B. Straumal, B. Baretzky, A.A. Mazilkin, F. Phillipp, O.A. Kogtenkova, M.N. Volkov and R.Z. Valiev: *Acta Mater.* Vol. 52 (2004), p. 4469
- [3] A.A. Mazilkin, O.A. Kogtenkova, B.B. Straumal, R.Z. Valiev and B. Baretzky: *Def. Diff. Forum Vols.* 237–240 (2005), p. 739
- [4] Ch. Xu, M. Furukawa, Z. Horita and T.G. Langdon: *Acta Mater.* Vol. 53 (2005), p. 749
- [5] G.K. Williamson and W.H. Hall: *Acta Metall.* Vol. 1 (1953), p. 22
- [6] T. Ungár and A. Borbely: *Appl. Phys. Lett.* Vol. 69 (1996), p. 3173
- [7] T. Ungár, S. Ott, P. Sanders, A. Borbely and J.R. Weertman: *Acta Mater.* Vol. 46 (1998), p. 3693
- [8] T.B. Massalski et al. eds: *Binary Alloy Phase Diagrams* (ASM International, Materials Park 1993)
- [9] J. Meissner: *Zt. Metallkd.* Vol. 50 (1959), p. 207
- [10] F. Pfaff: *Zt. Metallkd.* Vol. 53 (1962), p. 411
- [11] E.O. Hall: *Proc. Phys. Soc. B* Vol. 64 (1951), p. 747
- [12] N.J. Petch: *J. Iron Steel Inst.* Vol. 173 (1953), p. 25
- [13] N.L. Peterson and S.J. Rothman: *Phys. Rev. B* Vol. 1 (1970), p. 3264
- [14] I. Gödény, D.L. Beke and F.J. Kedves: *Phys. Stat. Sol. (a)* Vol. 13 (1972), p. K155
- [15] S.J. Rothman, N.L. Peterson, L.J. Nowicki and L.C. Robinson: *Phys. Stat. Sol. B* Vol. 63 (1974), K 29
- [16] G. Saada: *Acta Met.* Vol. 9 (1961), p. 965
- [17] D.L. Beke, I. Gödény and F.J. Kedves: *Phil. Mag. A* Vol. 47 (1983), p. 281
- [18] D.L. Beke, I. Gödény and F.J. Kedves: *Trans. Jap. Inst. Met. Suppl.* Vol. 27 (1986), p. 649
- [19] P. Zieba, A. Pawlowski and W. Gust: *Def. Diff. Forum* Vol. 194 (2001), p. 1759
- [20] T. Fujita, H. Hasegawa, Z. Horita and T.G. Langdon: *Def. Diff. Forum* Vol. 194 (2001), p. 1205
- [21] T. Fujita, Z. Horita and T.G. Langdon: *Phil. Mag A* Vol. 82 (2002), p. 2249